Molecular Hydrogen Absorption in the z = 1.97 Damped Lyα Absorption System toward QSO 0013−004[1]

Jian Ge & Jill Bechtold

Steward Observatory, University of Arizona, Tucson, AZ 85721

Received _____; accepted _____

[1]Observations here were obtained with the Multiple Mirror Telescope, a joint facility of the University of Arizona and the Smithsonian Institution.

ABSTRACT

We present a new ultra-violet spectrum of the QSO 0013−004 with 0.9 Å resolution obtained with the MMT Blue spectrograph. The v = 0 - 0, 1 - 0, 2 - 0 and 3 - 0 Lyman bands of H_2 associated with the z = 1.9731 damped Lyα absorption line system have been detected. The H_2 column density is N(H_2) = 6.9($\pm$1.6) $\times$ 10^{19} cm^{-2}, and the Doppler parameter b = 15$\pm$2 km s^{-1}. The populations of different rotational levels are measured and used to derive the excitation temperatures. The estimated kinetic temperature $T_K \sim 70$ K, and the total particle number density $n(H) \sim 300$ cm^{-3}. The UV photoabsorption rate $\beta_0 \sim 6.7 \times 10^{-9}$ s^{-1}, about a factor of few times greater than that in a typical diffuse Milky Way interstellar cloud. The total hydrogen column density is N(H) = 6.4($\pm$0.5) $\times$ 10^{20} cm^{-2}. The fractional H_2 abundance f = 2N(H_2)/(2N(H_2) + N(H I)) $\sim$ 0.22 $\pm$ 0.05 is the highest among all observed damped Lyα absorbers. The high fractional H_2 abundance is consistent with the inferred presence of dust and strong C I absorption in this absorber.

Subject headings: ISM: molecules – quasars: absorption lines – quasars: individual (Q0013−004)

1. Introduction

Damped Lyα quasar absorption line systems are commonly believed to trace a population of objects which may be the progenitors of modern galaxies (e.g. Wolfe 1990). The typical metallicity and dust-to-gas ratio in the damped Lyα systems at z $\sim$ 2 is measured to be about 10% of those in the Milky Way with a large scatter (e.g. Pettini *et al.* 1994; 1995; Pei, Fall & Bechtold, 1991; Lu *et al.* 1996). The UV Lyman and Werner bands of H_2 have been difficult to detect however, so that little is known about molecular gas in damped Lyα galaxies (Levshakov *et al.* 1992; Lanzetta *et al.* 1989; Foltz et al 1988; Chaffee *et al.* 1988; Black *et al.* 1987). The problem such searches face is that without high resolution and high signal-to-noise ratio spectra, the molecular hydrogen lines are blended with the Lyα forest lines. Further, quasar absorption line studies usually concentrate on bright blue quasars, so lines of sight with substantial reddening and large molecular fraction are probably selected against (Ostriker & Heisler, 1984; Fall & Pei 1993). So far, there is only one detection of H_2 absorption in the z = 2.811 damped Lyα absorber toward PSK 0528−250, which shows moderate H_2 absorption with total column density $N(H_2) = 1 \times 10^{18}$ cm^{-2} (Foltz *et al.* 1988; Lanzetta 1993). This system may not be representative since its redshift is very close to the redshift of the quasar.

Previous observations of the $z_{ab} = 1.9731$ damped Lyα absorber toward Q 0013−004 ($z_{em} = 2.0835$) showed C I absorption, and line ratios of Cr II, Fe II and Zn II indicated significant depletion, and hence a relatively high dust-to-gas ratio compared to other damped Lyα absorbers (Pettini et al. 1994, Ge, Bechtold, & Black 1996). Thus, it seemed to be a good system to search for H_2. In this *Letter*, we report the detection of strong H_2 absorption lines.

2. Observations

Spectra were obtained with the Multiple Mirror Telescope (MMT) on Oct. 13 and Oct. 24 - 25, 1995 with the Blue Channel Spectrograph and the Loral 3072×1024 CCD. The 832 l/mm grating was used in second order. A $1'' \times 180''$ slit was used to give a resolution of 0.9 Å, corresponding to 2.6 pixels, measured from the comparison lamp lines. The wavelength coverage was from 3000 Å to 4100 Å. The seeing was $1.0''$ (FWHM). The integration was composed of twelve separate exposures of 50 minutes each. The QSO was stepped by a few arcseconds along the slit between each exposure to smooth out any residual irregularities in the detector response which remained after flat-fielding. An exposure of a He-Ne-Ar-Cu lamp was done before and after each exposure of the object to provide an accurate wavelength reference, and a measure of the spectral resolution. Several quartz lamp exposures were taken at the beginning and end of the nights to provide a flat-field correction. We also observed standard stars before and after the QSO observations to monitor possible atmospheric absorption.

The data were reduced in the standard way using IRAF. The He-Ne-Ar-Cu spectra were extracted with the same procedure and a first order Spline3 function fit was used to obtain a wavelength calibration. The root-mean-square residuals to the wavelength fit are typically 0.05 Å. All reported wavelengths are vacuum and have been corrected to the heliocentric frame. We have rebined pixels in the common wavelength ranges of the spectra from the two observation runs and combined them, weighted by the signal-to-noise ratio (S/N). Part of the summed spectra are shown in Figures 1(a) and 2. The S/N is ~ 10 per pixel in the wavelength range of 3150 - 3350 Å, which covers the H_2 absorption bands. The S/N ~ 20 or higher in the wavelength range of 3500 - 3750 Å, which covers the damped Lyα absorption. The continuum was fitted in the way described by Bechtold (1994). The spectra shown were normalized by their fitted continuum.

3. Results

Fig. 1(a) shows the spectral region containing the H_2 Lyman v = 0 - 0, 1 - 0, 2 - 0 and 3 - 0 bands for the z = 1.9731 damped Lyα absorber. A simulated spectrum of the H_2 Lyman bands is plotted as a dotted line for comparison. There is remarkable agreement between the two spectra despite the presence of Lyα forest lines.

In order to investigate whether the observed configuration of lines is the result of chance coincidence with Lyα forest lines, we cross-correlated the observed spectrum (3150 - 3350 Å) with the simulated H_2 absorption line spectrum (3150 - 3350 Å) using FXCOR in IRAF (see Tonry & Davis 1979 section III for details; Foltz et al., 1988). The cross-correlation function was computed for lags in the range $-16{,}000 \leq \Delta v \leq 16,000$ km s^{-1} and is shown in Fig. 1(b). A very strong peak with the correlation amplitude of 0.66 is noted near zero velocity shift. The other two second strong peaks at $\sim \pm$ 4,300 km s^{-1} are caused by shifting the spectra by one band separation ($\sim$ 47 Å in the observed frame, e.g. Morton & Dinerstein, 1976). If the regions in the spectrum around the four identified strong Lyα and metal lines, as marked in Fig. 1(a) (3216.2 - 3224.9 Å, 3296.1 - 3300.3 Å), are removed from the data before the correlation was carried out, the peak correlation amplitude is 0.82. The measured redshift for the H_2 absorption corresponding to the peak position of the cross-correlation function, $z_{H_2} = 1.9731$, is consistent with the redshift of the metal lines (Ge *et al.* 1997).

In order to estimate the statistical significance of the correlation amplitude, we have simulated Lyα forest line spectra using the program described in Dobrzycki & Bechtold (1996). In order to be conservative, we made synthetic spectra that matched the total absorption line density of all the strong lines in the Q 0013−004 spectrum between 3150 and 3350 Å even though several of the strong lines are actually metal transitions for the z = 1.97 system. We cross-correlated 1000 simulated spectra with the synthetic H_2 absorption

line spectrum. The peak values of the cross-correlation function are all smaller than 0.55. Thus, the probability of obtaining a correlation peak of 0.66 by chance is less than 10^{-4}.

To obtain column densities from the measured values of equivalent width (Table 1), a curve-of-growth was constructed for J = 2, 3, 4, 5 rotational levels (Fig. 3). The theoretical curves for the 0-0 Lyman band with different Doppler b-values, b = 10, 13, 15, 17, 20 km s^{-1}, are shown. Absorption lines for J = 4, 5 are on the linear section. Absorption lines from J = 2, 3 are on the flat section. The observed values for J = 2, 3, 4 and 5 are consistent with b = 15±2 km s^{-1}. Table 2 shows the derived column densities for J = 2, 3, 4 assuming the b = 15±2 km s^{-1}, and upper limits for J = 5, 6, 7 assuming they are on the linear portion of the curve-of-growth. Column densities from J = 0, 1 are derived by the continuum-reconstruction procedure described by Savage *et al.* (1977), i.e. a reconstruction of the QSO spectrum was generated by dividing the observed spectrum by the synthetic H_2 spectrum of R(0), R(1), and P(1) lines. The final values of N(J=0) and N(J=1) were determined from the best-fit reconstructions of (2,0), (1,0) and (0,0) Lyman bands (Table 2). The uncertainties in the final column densities were estimated by the same procedure. Together, the total H_2 column density is $N(H_2) = 6.9(\pm1.6) \times 10^{19}$ cm^{-2}.

Table 2 also includes the derived excitation temperatures for the rotational levels. The measured $T_{01} = 70 \pm 13$ K is in the range of typical values of the Milky Way diffuse clouds (Savage *et al.* 1977) and also similar to the z = 2.811 damped Lyα absorber of PKS 0528−250 (Songaila & Cowie 1995). The $T_{02} = 82^{+17}_{-6}$ K is also in the range of the average value for the Milky Way clouds. The excitation temperatures for higher J, T_{ex}, of 200 - 500 K, are similar to that of Milky Way clouds (Spitzer *et al.* 1974).

Fig. 2 shows the observed damped Lyα profile and fits to the line profile. The neutral hydrogen column density $N(H\ I) = 5.0(\pm0.5) \times 10^{20}$ cm^{-2}, the Doppler parameter, $b_{HI} = 50$ km s^{-1} and $z_{HI} = 1.9731$. The neutral hydrogen absorption redshift is consistent with the

metal line and H_2 redshifts. The measured fractional H_2 abundance $f = 2N(H_2)/(2N(H_2) + N(H\ I)) = 0.22 \pm 0.05$, is about a factor of 60 times higher than that of the z = 2.811 damped Lyα system toward PKS 0528−250 and the limits for other damped systems previously searched for H_2 absorption (Black et al, 1987; Chaffee *et al.* 1988, Foltz *et al.* 1988; Lanzetta *et al.* 1989; Levshakov *et al.* 1992; Songaila & Cowie, 1996).

4. Discussion

The molecular fraction $f = 0.22 \pm 0.05$ for the z = 1.97 absorber is similar to that seen in $E(B - V) > 0.1$ clouds in the Milky Way (Savage *et al.* 1977). Indeed, the upper limit of the relative depletion of Cr to Zn, $[Cr/Zn] \leq -1.0$ (Pettini *et al.* 1994) suggests that the dust-to-gas ratio in this absorber is much higher than the average value of 10% of the Milky Way's ratio for damped systems at $z \sim 2$ (Pettini *et al.* 1994). The previous observation of Fe II λ 1608.45 Å provides a direct comparison of the relative depletion of Fe to Zn, $[Fe/Zn] = -1.2$ (Ge *et al.* 1997) to those of the Milky Way's diffuse clouds. Table 3 shows a comparison between the z = 1.9731 absorber and the diffuse clouds toward ζ Oph and ξ Per (Spitzer *et al.* 1974; Savage *et al.* 1977; Jura 1975; Savage *et al* 1992; Cardelli *et al.* 1991). The relative depletion of [Fe/Zn] implies that the dust-to-gas ratio in the z = 1.9731 absorber is $\sim 50\%$ of the Milky Way's value. The relatively normal dust-to-gas ratio is consistent with the high H_2 fraction because H_2 is very efficiently formed on dust grain surfaces (Savage *et al.* 1977).

As discussed by previous reviews (e.g. Spitzer & Jenkins, 1975; Shull & Beckwith 1982), the relative populations of J = 0 and 1 are established dominantly by thermal particle collisions, especially for saturated lines, so the excitation temperature, T_{01}, is approximately equal to the kinetic temperature, T_k, of the clouds. The measured $T_{01} = 70 \pm 13$ K in the z = 1.9731 absorber implies that the kinetic temperature is similar to that of the Milky

Way diffuse clouds, $\langle T_{01} \rangle = (77 \pm 17)$ K (Savage *et al.* 1977). The higher rotational levels are populated primarily by collisions, formation pumping and UV pumping and radiative cascade after photoabsorption to the Lyman and Werner bands (e.g. Spitzer & Zweibel 1974; Jura 1974, 1975). For example, the J = 4 is populated by direct formation pumping, and by UV pumping from J = 0 (e.g. Black & Dalgarno 1976). For densities less than 10^4 cm^{-3}, the J = 4 level is depopulated mainly by spontaneous emission (Dalgarno & Wright 1972; Elitzur & Watson 1978). Therefore, in a steady state for J = 4,

$$p_{4,0}\beta(0)n(H_2, J=0) + 0.19Rn(H)n = A_{42}n(H_2, J=4), \tag{1}$$

where $p_{4,0} = 0.26$ is the UV pumping efficiency into the J = 4 level from the J = 0 level (Jura 1975), $A_{42} = 2.8 \times 10^{-9}$ s^{-1} is the spontaneous transition probability (Dalgarno & Wright 1972), R is the H_2 formation rate, n = n(H) + 2n(H_2), and $\beta(J)$ denotes the rate of absorption in the Lyman and Werner bands from the Jth rotational level, including any attenuation (see Jura 1975 for details). The equilibrium between the H_2 formation on dust grains and H_2 destruction by absorption of Lyman- and Werner-band radiation (e.g. Jura 1975) can be written as

$$In(H_2) = Rn(H)n \approx 0.11 \sum_{J=0}^{6} \beta(J)n(H_2, J), \tag{2}$$

where I is the H_2 dissociation rate (Jura 1975). If the self-shielding in J = 0, 1 levels is about the same, so that $\beta(0) \approx \beta(1)$, then

$$n(H_2, J=4)A_{42} = 1.52Rn(H)n. \tag{3}$$

Thus, $Rn = 8.1(^{+3.9}_{-2.6}) \times 10^{-15}$ s^{-1} for the Q 0013−004 cloud, which is about the same magnitude as that for ξ Per and ζ Oph clouds (Jura 1975).

We can use the analytic calculation for n(H_2)/n(H) within a H_2 cloud by Jura (1974) to estimate the H_2 dissociation rate $I \approx 7.4 \times 10^{-10}$ s^{-1}. The photoabsorption rate in the

Lyman and Werner bands outside of the cloud, $\beta_0 \approx I/0.11 \approx 6.7 \times 10^{-9}$ s^{-1}, which is similar to that of ξ Per cloud (Jura 1975) and about a factor of a few higher than that of ζ Oph cloud (Federman *et al.* 1995). Further, the photoabsorption rate, β_0, depends linearly on the local radiation field at 930 - 1150 Å (Jura 1974), therefore, the β_0 for the z = 1.9731 absorber corresponds to an estimated local radiation field at 1000 Å of $J_{1000\mathring{A}} \approx 3 \times 10^{-18}$ ergs cm^{-2}s^{-1}Hz^{-1}ster^{-1}. Thus $J_{1000\mathring{A}}$ is about three orders of magnitude higher than the radiation field at the Lyman limit, $J_{912\mathring{A}}$, expected in the ambient IGM at this redshift (e.g. Lu *et al.* 1991; Bechtold 1994). The radiation field at 1000 Å is therefore probably dominated by the UV emission by hot stars in this galaxy.

As mentioned above, the z = 1.9731 absorber has a similar dust-to-gas ratio to that of the Milky Way diffuse clouds. If we assume the H_2 formation rate on grains, R $\sim 3 \times 10^{-17}$ cm^{3}s^{-1}, the typical rate for the Milky Way's clouds (Jura 1975), then the inferred value of the number density n $\sim$ 300 cm^{-3}, about the same as that of the ζ Oph and ξ Per clouds.

The derived values of the UV radiation field, density, and temperature in the z = 1.97 absorber are estimates based on the simple analysis of Jura (1975), which ignores the depth-dependence of the attenuation by dust and self-shielding of absorption lines. However, the results from this simple analysis are qualitatively consistent with that from more detailed modeling (e.g. van Dishoeck & Black 1986).

We note that there is some uncertainty in the derived b-value. While b = 15 km s^{-1} provides the best fit to the observed values, smaller Doppler parameters, for example, b = 2 km s^{-1}, also give an acceptable solution. In this case, the implied column densities in J = 2, 3 and 4 are so high they would suggest that conditions more like a photon-dominated region (PDR) are implied (e.g. Draine & Bertoldi 1996; Black & van Dishoeck 1987; Abgrall *et al.* 1992; Le Bourlet *et al.* 1993; Sternberg & Dalgarno 1989). The populations in J = 2, 3 and 4 would be fit by a single excitation temperature of 350 K. This would leave excess

population in J = 0 and 1, suggesting a cold component at $T_{01} \approx 63$ K. The density of the absorber cloud would have to be lower than ~ 5000 cm^{-3} in order for the J = 5 limit to be consistent with the populations in J = 2, 3 and 4.

Finally, if the larger value b = 15 km s^{-1} is correct, then this absorber has a b-value which is much larger than that for typical Milky Way diffuse clouds (e.g. Spitzer *et al.* 1974). This would indicate that there is likely more than one velocity component. Spectra of higher resolution would permit a better constrained analysis of the excitation and molecular abundance and provide a better understanding of physical conditions in this high redshift galaxy.

We thank Dr. John Black for providing his H_2 absorption line synthesis code and helpful discussions. We thank Dr. Adam Dobrzycki for use of his spectral synthesis code. We thank Dr. Dave Meyer for helpful conversations. We thank the staff of MMTO for their help. This research was supported by NSF AST-9058510.

REFERENCES

Abgrall, H., Le Bourlot, J., Pineau des Forets, G., Roueff, E., Flower, D.R., & Heck, L., 1992, A&A, 253, 525

Bechtold, J., 1994, ApJS, 91, 1

Bergeson, S.D., & Lawler, J.E. 1993, ApJ, 408, 382

Black, J.H., & Dalgarno, A. 1976, ApJ, 203, 132

Black, J. H., Chaffee, F. H. Jr., & Foltz, C. B., 1987, ApJ, 317, 442

Black, J.H., & van Dishoeck, E.F., 1987, 322, 412

Cardelli, J.A. *et al.* 1991, ApJ, 377, L57

Chaffee, F.H., Foltz, C.B., & Black, J.H. 1988, ApJ, 335, 584

Dalgarno, A., & Wright, E.L. 1972, ApJ, 174, L49

Dobrzycki, A., & Bechtold, J. 1996, ApJ, 457, 102

Draine, B.T., & Bertoldi, F., 1996, ApJ, 468, 269

Elitzur, M., & Watson, W.D. 1978, A&A, 70, 443

Fall, S.M., & Pei, Y.C. 1993, ApJ, 402, 479

Federman, S.R., Cardelli, J.A., van Dishoeck, E.F., Lambert, D.L., & Black, J.H., 1995, ApJ, 445, 325

Foltz, C. B., Chaffee, F. H., & Black, J. H. 1988, ApJ, 324, 267

Ge, J., Bechtold, J. & Black, J.H. 1997, ApJ, 474, 67

Jura, M. 1974, ApJ, 191, 375

Jura, M. 1975, ApJ, 197, 581

Lanzetta, K. M., Wolfe, A. M., Turnshek, D. A. 1989, ApJ,344, 277

Lanzetta, K. M. 1993, in The Enviroment and Evolution of Galaxies, eds: J. M. Shull & H. A. Thronson, Jr. (Kluwer Academic Publishers), 237

Le Bourlot, J., Pineau des Forets, G., Roueff, E., & Flower, D.R., 1993, A&A, 267, 233

Levshakov, S.A., Chaffee, F.H., Foltz, C.B., & Black, J.H. 1992, A&A, 262, 385

Lu, L., Wolfe, A.M., & Turnshek, D.A. 1991, ApJ, 367, 19

Lu, L. 1996 in Cosmic Abundances, ASP Conference Series, eds. S.S. Holt, & G. Sonneborn, Vol. 99, 105

Morton, D.C., & Dinerstein, H.L. 1976, ApJ, 204, 1

Ostriker, J.P., & Heisler, J. 1984, ApJ, 278, 1

Pei, Y. C., Fall, S. M. & Bechtold, J. 1991, ApJ, 378, 6

Pettini, M., Smith, L. J., Hunstead, R. W., & King, D. L., 1994, ApJ, 426, 79

Pettini, M., King, D. L., Smith, L. J., & Hunstead, R. W. 1995, in QSO absorption lines, ed. G. Meylan (Springer-Verlag)

Savage, B.D., Bohlin, R.C., Drake, J.F. & Budich, W. 1977, ApJ, 216, 291

Savage, B.D., Cardelli, J.A., & Sofia, U.J. 1992, ApJ, 401, 706

Shull, J.M., & Beckwith, S. 1982, ARA&A, 20, 163

Songaila, A., & Cowie, L. L. 1995, AJ, submitted

Spitzer, L., Cochran, W.D., & Hirshfeld, A. 1974, ApJS, 28, 373

Spitzer, L., & Zweibel, E.G. 1974, ApJ, 191, L127

Spitzer, L., & Jenkins, E.B. 1975, ARA&A, 13, 133

Sternberg, A., & Dalgarno, A., 1989, ApJ, 338, 197

Tonry, J., & Davis, M. 1979, AJ, 84, 1511

van Dishoeck, E.F., & Black, J.H., 1986, ApJS, 62, 109

Wolfe, A. M. 1990, in the Interstellar Medium in Galaxies, eds. H.A. Thronson & J.M. Shull (Kluwer, Dordrecht), 387

Table 1. H_2 absorption lines in the z = 1.9731 damped Lyα absorber

No.	λ_{rest}(Å)	λ_{obs}(Å)	W_{obs}(Å)	z_{abs}	ID
1	1062.883	3158.63±0.20	$\geq$3.02[a]	1.9718	L3-0 R(0)
2	1063.460	3161.85±0.10	$\geq$2.74[a]	1.9732	L3-0 R(1)
3	1064.606	3165.01±0.12	$\geq$1.47[a]	1.9729	L3-0 P(1)
4	1064.995	3166.94±0.30	0.77±0.16	1.9737	L 3-0 R(2)
5	1066.901	3171.78±0.11	0.79±0.15	1.9729	L 3-0 P(2)
6	1067.478	3173.80±0.11	0.79±0.15	1.9732	L 3-0 R(3)
7	1070.142	3182.18±0.10	0.74±0.12	1.9736	L 3-0 P(3)
8	1070.898	3184.14±0.19	0.33±0.10	1.9733	L 3-0 R(4)
9	1074.313	3194.04	$\leq$ 0.202[b]	1.9731	L 3-0 P(4)
10	1085.382	3226.95	$\leq$ 0.248[b]	1.9731	L 3-0 P(6)
11	1086.626	3230.65	$\leq$ 0.256[b]	1.9731	L 3-0 R(7)
12	1077.138	3202.32±0.10	$\geq$1.99[a]	1.9730	L 2-0 R(0)
13	1077.678	3204.27±0.10	$\geq$2.02[a]	1.9733	L 2-0 R(1)
14	1078.926+1079.226	3208.14±0.10	1.89±0.20	1.9731	L 2-0 P(1)+R(2)
15	1081.265	3214.68±0.07	0.87±0.10	1.9731	L 2-0 P(2)
16	1088.794	3237.09	$\leq$ 0.20[b]	1.9731	L 2-0 P(4)
17	1100.016	3270.46	$\leq$ 0.22[b]	1.9731	L 2-0 P(6)
18	1092.194	3247.02±0.14	$\geq$2.38[a]	1.9729	L 1-0 R(0)
19	1092.732	3249.27±0.08	$\geq$2.05[a]	1.9735	L 1-0 R(1)
20	1094.052+1094.244	3253.13±0.06	2.08±0.14	1.9731	L 1-0 P(1)+R(2)
21	1099.788	3269.66±0.08	0.66±0.09	1.9730	L 1-0 P(3)
22	1100.165	3270.90	$\leq$ 0.22[b]	1.9731	L 1-0 R(4)
23	1104.084	3282.24±0.18	0.18±0.07	1.9728	L 1-0 P(4)
24	1104.547	3283.93	$\leq$ 0.16[b]	1.9731	L 1-0 R(5)
25	1108.128+1108.634	3295.23	$\geq$2.04[a]	1.9731	L 0-0 R(0)+R(1)
26	1112.495+1112.584	3207.59	1.25±0.13	1.9731	L 0-0 P(2)+R(3)
27	1120.246+1120.399	3331.10	0.34±0.08	1.9731	L 0-0 P(4)+R(5)
28	1125.539+1125.725	3346.65	$\leq$ 0.16[b]	1.9731	L 0-0 P(5)+R(6)

[a] Lower limits due to the probable existence of the damping wings of these lines

[b] 2σ upper limits

Table 2. H_2 Column Densities and Excitation Temperatures in the z = 1.9731 Damped Lyα Absorber

Level	N(cm^{-2})[a]	T_{ex}(K)	J_{ex}
J = 0	$3.8(\pm1.2) \times 10^{19}$		
J = 1	$3.0(\pm1.0) \times 10^{19}$	70 ± 13	0-1
J = 2	$3.8^{+4.8}_{-1.1} \times 10^{17}$	82^{+17}_{-6}	0-2
J = 3	$1.4^{+2.1}_{-0.6} \times 10^{17}$	208^{+168}_{-44}	2-3
J = 4	$2.5^{+1.2}_{-0.8} \times 10^{15}$	209^{+50}_{-16}	2-4
J = 5	$\leq 1.6 \times 10^{15}$	≤ 271	2-5
J = 6	$\leq 1 \times 10^{15}$	≤ 430	2-6
J = 7	$\leq 9 \times 10^{14}$	≤ 497	2-7

[a] 2σ upper limits given for J = 5, 6, 7

Table 3. Comparison between the z = 1.9731 Absorber and ζ Oph and ξ Per clouds

Name	lg N(H_2) (cm^{-2})	lg N(H I) (cm^{-2})	lg f	[Zn/H]	[Fe/H]	T_{01} (K)	T_{02} (K)	T_{ex} (K)	n(H) (cm^{-3})	β_0 ($10^{-10}s^{-1}$)	b (km s^{-1})
Q 0013	19.86 ± 0.10	20.70±0.05	−0.66 ± 0.10	-0.80 ± 0.08[c]	−1.95±0.01	70 ± 13	82^{+17}_{-8}	200-500	∼ 300	∼ 67	15 ± 2
ζ Oph[a]	20.65	20.72	−0.20	> −0.81	−2.38	54	84	324	700	∼ 10^{d}	3.8
ξ Per[b]	20.53	21.11	−0.46	−0.65	−2.24	71	78	384	300	50	5

[a] Results are from Spitzer *et al.* 1974; Savage *et al.* 1977; Jura 1975; Savage *et al.* 1992.

[b] Data are from Spitzer *et al.* 1974; Savage *et al.* 1977; Jura 1975; Cardelli *et al.* 1991.

[c] Based on the f-value from Bergeson *et al.* (1993)

[d] Federman *et al.* (1995)

Figure Captions

Figure 1. – (a). Spectrum of QSO 0013−004 obtained with the MMT Blue Channel Spectrograph. The dotted line is the synthetic absorption line spectrum of the v = 0 - 0, 1 - 0, 2 - 0 and 3 - 0 Lyman bands associated with the z = 1.9731 damped Lyα absorber. Strong absorption lines No. 1, 2, 3 are identified as N II λ 1083.99 Å at z = 1.9673, 1.9714, 1.9731, respectively, consistent with other metal line identifications (Ge *et al.* 1997). The strong line No. 4 is identified as H I Lyα line at z = 1.7135, which shows C IV $\lambda\lambda$ 1548,1550 lines in previous observed QSO spectra (Ge *et al.* 1997). (b). Cross correlation between the QSO spectrum and the synthetic H_2 absorption line spectrum shown in Fig. 1. The peak near zero velocity has the largest amplitude in the testing range −16,000 to 16,000 km s^{-1}. The two second highest peaks are evidently caused by shifting two spectra with one Lyman band separation ($\sim$ 47 Å at the observed frame).

Figure 2. – The damped Lyα absorption line at z = 1.9731. The three curves are profiles with $N(HI) = (4.5, 5.0, 5.5) \times 10^{20}$ cm^{-2} and b = 50 km s^{-1}.

Figure 3. – Curves of growth for H_2 (0,0) Lyman band with b = 10, 13, 15, 17 and 20 km s^{-1}. The lines from J = 4, 5 are on the linear part, while those from J = 2, 3 are on the flat part of the curve of growth. All lines are consistent with b = 15$\pm$2 km s^{-1}.

Fig. 1

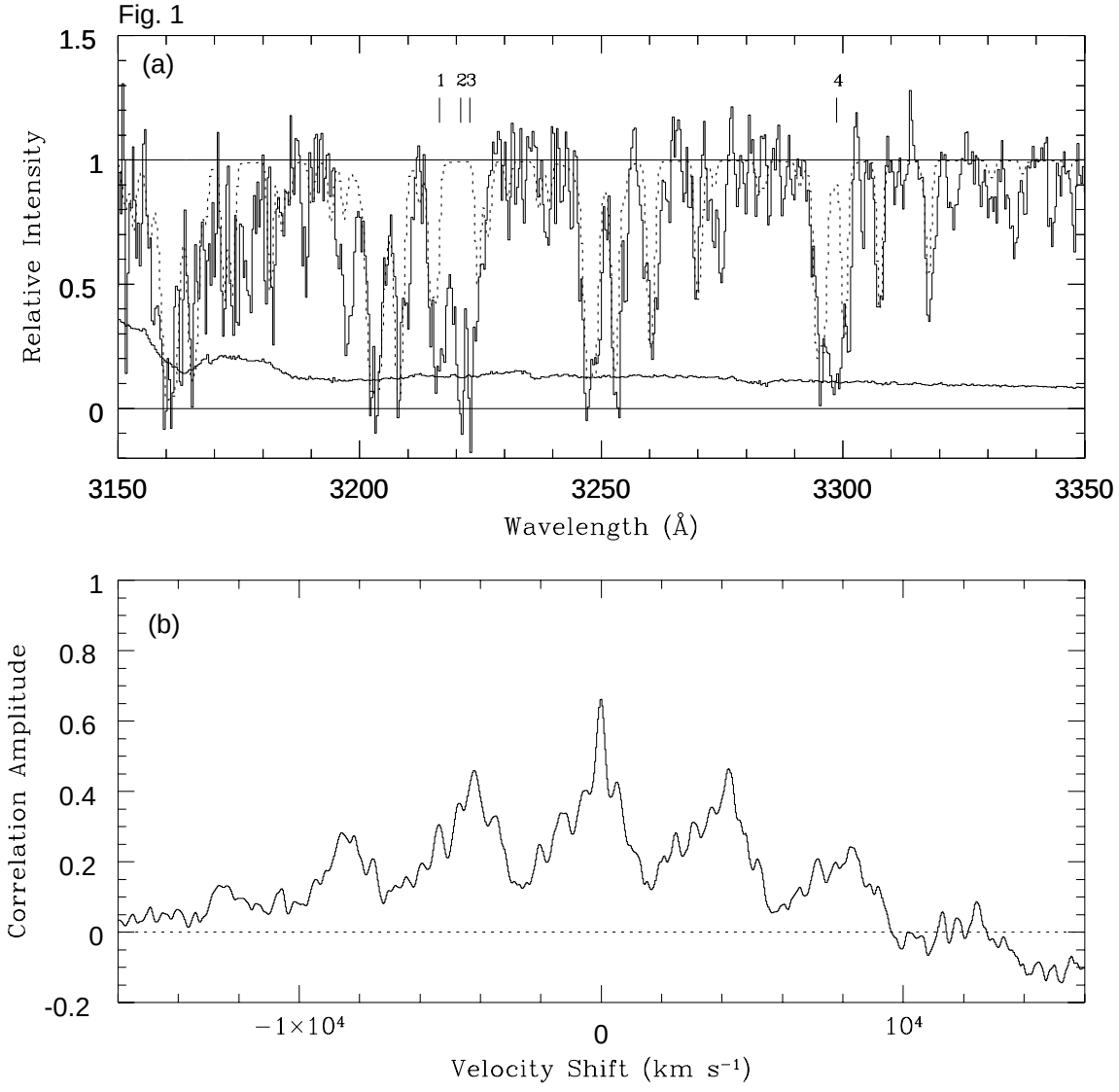
(a)
1 23
4
1.5
1
0.5
0
Relative Intensity
3150
3200
3250
3300
3350
Wavelength (Å)
(b)
1
0.8
0.6
0.4
0.2
0
-0.2
Correlation Amplitude
−1×10⁴
0
10⁴
Velocity Shift (km s⁻¹)

Fig. 2

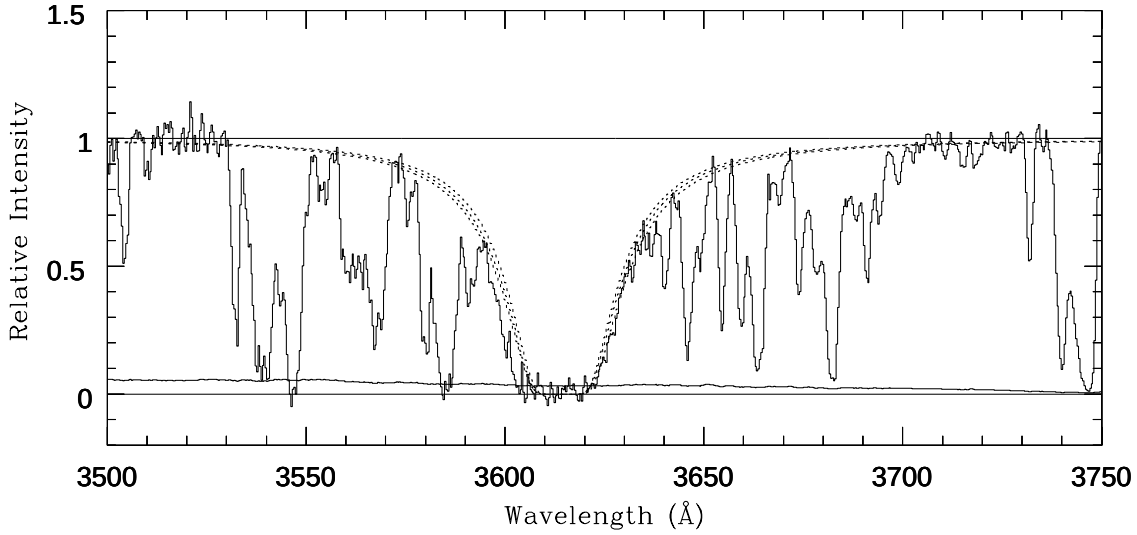
1.5
1
0.5
0
Relative Intensity
3500
3550
3600
3650
3700
3750
Wavelength (Å)

Fig. 3

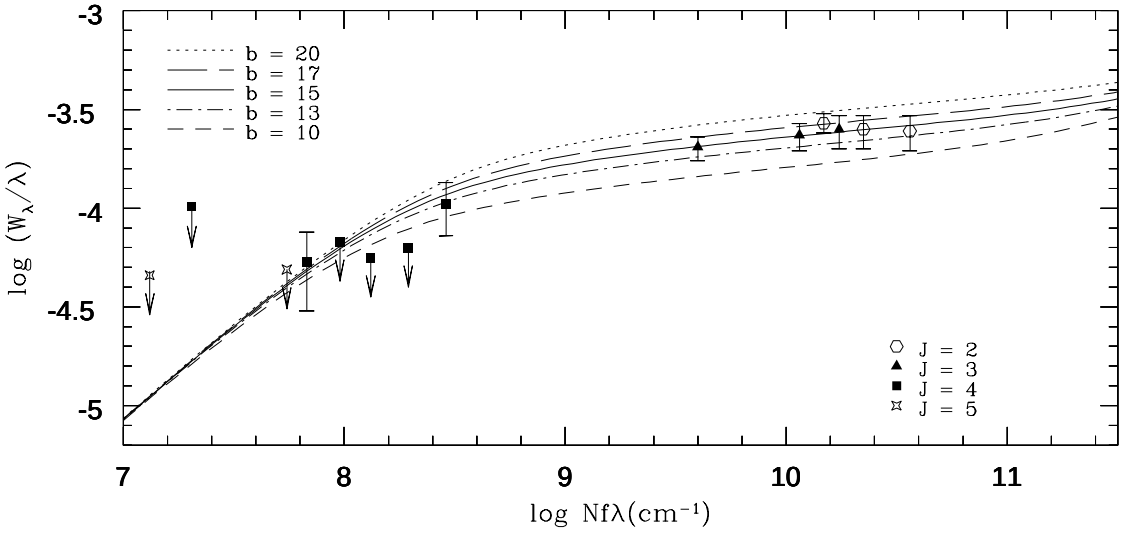
b = 20
b = 17
b = 15
b = 13
b = 10
J = 2
J = 3
J = 4
J = 5
log (W_λ/λ)
log Nfλ(cm⁻¹)
-3
-3.5
-4
-4.5
-5
7
8
9
10
11